



**HAL**  
open science

## **Turnip mosaic virus is a second example of a virus using transmission activation for plant-to-plant propagation by aphids**

Edwige Berthelot, Marie Ducousso, Jean Luc Macia, Florent Bogaert, Volker Baecker, Gael Thébaud, Romain Gallet, Michel Yvon, Stéphane Blanc, Mounia Khelifa, et al.

### **► To cite this version:**

Edwige Berthelot, Marie Ducousso, Jean Luc Macia, Florent Bogaert, Volker Baecker, et al.. Turnip mosaic virus is a second example of a virus using transmission activation for plant-to-plant propagation by aphids. *Journal of Virology*, 2019, 93 (9), pp.e01822-18. 10.1128/JVI.01822-18 . hal-02478112

**HAL Id: hal-02478112**

**<https://hal.umontpellier.fr/hal-02478112>**

Submitted on 13 Mar 2020

**HAL** is a multi-disciplinary open access archive for the deposit and dissemination of scientific research documents, whether they are published or not. The documents may come from teaching and research institutions in France or abroad, or from public or private research centers.

L'archive ouverte pluridisciplinaire **HAL**, est destinée au dépôt et à la diffusion de documents scientifiques de niveau recherche, publiés ou non, émanant des établissements d'enseignement et de recherche français ou étrangers, des laboratoires publics ou privés.

1 Turnip mosaic virus is a second example of a virus using transmission  
2 activation for plant-to-plant propagation by aphids

3 Edwige Berthelot <sup>a,b,c</sup>, Marie Ducouso <sup>a</sup>, Jean-Luc Macia <sup>a</sup>, Florent Bogaert <sup>d</sup>, Volker Baecker <sup>e</sup>,  
4 Gaël Thébaud <sup>a</sup>, Romain Gallet <sup>a</sup>, Michel Yvon <sup>a</sup>, Stéphane Blanc <sup>a</sup>, Mounia Khelifa <sup>b,c,#</sup>, Martin  
5 Drucker <sup>a,d,#</sup>

6 <sup>a</sup> BGPI, INRA Centre Occitanie, SupAgro, CIRAD, Université de Montpellier, Montpellier,  
7 France

8 <sup>b</sup> Semences Innovation Protection Recherche et Environnement, Achicourt, France

9 <sup>c</sup> Fédération Nationale des Producteurs de Plants de Pomme de Terre, Paris, France

10 <sup>d</sup> SVQV, INRA Centre Grand Est, Université de Strasbourg, Colmar,

11 <sup>e</sup> France Montpellier Ressources Imagerie, Biocampus Montpellier, CNRS, INSERM, Université  
12 de Montpellier, Montpellier, France<sup>#</sup>

13 Corresponding authors. E-mail [mounia.khelifa@u-picardie.fr](mailto:mounia.khelifa@u-picardie.fr) and [martin.drucker@inra.fr](mailto:martin.drucker@inra.fr)

## 14 **Abstract**

15 Cauliflower mosaic virus (CaMV, family *Caulimoviridae*) responds to the presence of aphid vectors  
16 on infected plants by forming specific transmission morphs. This phenomenon, coined  
17 transmission activation (TA), controls plant-to-plant propagation of CaMV. A fundamental  
18 question is whether other viruses rely on TA. Here, we demonstrate that transmission of the  
19 unrelated Turnip mosaic virus (TuMV, family *Potyviridae*) is activated by the reactive oxygen  
20 species H<sub>2</sub>O<sub>2</sub> and inhibited by the calcium channel blocker LaCl<sub>3</sub>. H<sub>2</sub>O<sub>2</sub>-triggered TA manifested  
21 itself by the induction of intermolecular cysteine bonds between viral HC-Pro molecules and by  
22 formation of viral transmission complexes, composed of TuMV particles and HC-Pro that  
23 mediates vector-binding. Consistently, LaCl<sub>3</sub> inhibited intermolecular HC-Pro cysteine bonds and  
24 HC-Pro interaction with viral particles. These results show that TuMV is a second virus using TA  
25 for transmission, but using an entirely different mechanism than CaMV. We propose that TuMV  
26 TA requires ROS and calcium signaling and that it is operated by a redox switch.

## 27 **Importance**

28 Transmission activation, i.e. a viral response to the presence of vectors on infected hosts that  
29 regulates virus acquisition and thus transmission, is an only recently described phenomenon. It  
30 implies that viruses contribute actively to their transmission, something that has been shown  
31 before for many other pathogens but not for viruses. However, transmission activation has been  
32 described so far for only one virus, and it was unknown whether other viruses rely also on  
33 transmission activation. Here we present evidence that a second virus uses transmission  
34 activation, suggesting that it is a general transmission strategy.

## 35 **Key words**

36 Plant virus; aphid vector; host plant; virus transmission; virus vector host interactions; reactive  
37 oxygen species; calcium; signaling

## 38 **Abbreviations**

39 CaMV, cauliflower mosaic virus; TuMV, turnip mosaic virus; TA, transmission activation; ROS,  
40 reactive oxygen species; TB, transmission body; HC, helper component; HC-Pro, helper  
41 component protease; CP, capsid protein

## 42 Introduction

43 Transmission is an obligatory step in the life cycle of parasites but it is also an Achilles's heel,  
44 because parasites must leave the comparably comfortable environment of the host they are  
45 installed in, and face a potentially adverse environment during the passage to a new host. Some  
46 pathogens rely on resistant dormant states like spores to persist in the "wild" until they reach a  
47 new host passively, e.g. carried by the wind. Most pathogens, however, actively use vectors for  
48 transmission and they can manipulate both hosts and vectors in an impressive number of ways,  
49 all potentially increasing transmission (1–4). In the most sophisticated cases, pathogens "*use*  
50 *exquisitely controlled mechanisms of environmental sensing and developmental regulation to ensure their*  
51 *transmission*" (5). This concept, implying active contribution of the pathogen, is widely accepted  
52 for eukaryotic parasites (for example plasmodium, shistosoma, wucheraria, microcoelium), which  
53 developed fascinating transmission cycles to control and adapt vector-host or primary-secondary  
54 host interactions for their propagation (4). We have recently discovered a remarkable  
55 phenomenon for a virus. Cauliflower mosaic virus (CaMV, family *Caulimoviridae*) responds to the  
56 presence of aphid vectors on infected host plants by forming transmission morphs at the exact  
57 time and location of the plant-aphid contact (6). This process, coined Transmission Activation or  
58 TA (7), is characterized by the formation of transmission complexes between CaMV virus  
59 particles and the transmission helper component (HC), the CaMV protein P2, which mediates  
60 vector-binding (1). P2 and virus particles are spatially separated in infected cells since the cell's  
61 pool of P2 is retained in specific cytoplasmic inclusions called transmission bodies (TBs) while  
62 most virus particles are contained in another type of viral inclusion, the virus factories (8, 9). In  
63 such cells, aphid punctures trigger instant disruption of TBs and the liberated P2 relocates onto  
64 microtubules. Simultaneously, the virus factories release virus particles that associate with P2 on  
65 the microtubules (10) to form P2/virus particle complexes, which is the virus form that aphid  
66 vectors can acquire and transmit. TA is transient; P2 reforms a new TB (6) and the virus particles  
67 return to virus factories (10) after aphid departure. TA implies that CaMV passes, induced by yet  
68 unknown mechanisms, from a non-transmissible to a transmissible state. It has been suggested  
69 that this phenomenon exists to economize host resources and to invest energy in transmission  
70 only when relevant, i.e. in the presence of vectors (7). Whether this hypothesis is true or not,  
71 inhibiting TA inhibits transmission, pointing to the importance of TA for CaMV. A fundamental  
72 question that arises is whether TA, which is reminiscent of the active transmission strategies  
73 employed by eukaryotic parasites, is exclusive to CaMV or whether it could be a general  
74 phenomenon in the virus world. Therefore, we studied transmission of the turnip mosaic virus  
75 (TuMV, family *Potyviridae*), which is entirely unrelated to CaMV, but uses also an HC for aphid

76 transmission. The HC of TuMV and of other potyviruses is the viral protein helper component  
77 protease (HC-Pro). It is a multifunctional protein that other its HC function bears no structural,  
78 functional or other similarity with P2. Our results show that TuMV is a second virus relying on  
79 TA for transmission, but using a totally different mechanism.

## 80 **Results and discussion**

### 81 *Signaling molecules modify TuMV transmission by aphids*

82 TA requires a signaling cascade that connects the initial recognition of the presence of aphids,  
83 most likely via a yet unknown elicitor, with a cellular response that is hijacked by the virus. Since  
84 TA is fast for CaMV and likely also for TuMV, which uses the same transmission mode, reactive  
85 oxygen species (ROS) or calcium are good signaling candidates. We therefore tested the effect of  
86 the ROS signaling compound hydrogen peroxide ( $H_2O_2$ ), and of a general inhibitor of calcium  
87 signaling, lanthanum(III)chloride ( $LaCl_3$ ), on TuMV transmission, using infected protoplasts as  
88 virus source (6, 11). Aphid transmission tests performed with  $H_2O_2$ -treated protoplasts showed a  
89 drastic increase of TuMV transmission (Figure 1A) whereas treatment of protoplasts with  $LaCl_3$   
90 caused a strong reduction of transmission (Figure 1B). This effect was not due to modified cell  
91 viability (Figure 1C,D). Furthermore, transmission increase by  $H_2O_2$  and inhibition by  $LaCl_3$  was  
92 clearly a biological effect requiring living cells, since no effect was observed when the  
93 experiments were repeated using cell extracts, i.e. dead cells (Figure 1E,F). The same control  
94 experiments indicate also that  $H_2O_2$  and  $LaCl_3$  did not modify aphid feeding behavior, which  
95 might have been an alternative explanation for the observed differences in transmission rates.  
96 Taken together, our data show that TuMV transmission can be artificially enhanced or inhibited.

97 The protoplast system is a useful but simplified biological system because the cells are  
98 individualized and not in their natural symplasmic context in a tissue. Hence, we sought to  
99 validate the protoplast results by using leaves on intact infected plants as virus source. We applied  
100  $H_2O_2$  or  $LaCl_3$  to leaves by spraying treatment (12) and used these plants for aphid transmission  
101 assays. To rule out any interference, only one leaf of the same developmental stage was sprayed  
102 on each plant and different plants were used for each condition.  $H_2O_2$  treatment increased  
103 significantly and  $LaCl_3$  treatment decreased significantly plant-to-plant transmission rates of  
104 TuMV (Figure 1G,H). This confirmed the results obtained with protoplasts and showed that  
105 TuMV TA is observed similarly in intact plants. Compared to the protoplast experiments, higher  
106  $H_2O_2$  and  $LaCl_3$  concentrations were required to observe significant effects. This was probably  
107 due to dilution of these substances during leaf penetration. Combined, these results suggest that

108 the TA phenomenon exists for TuMV, like for CaMV, and that calcium and ROS signaling might  
109 be important for TA of TuMV.

110 *The increase in virus transmission correlates with the formation of HC-Pro/TuMV transmissible complexes*

111 Next, we wanted to know how TuMV TA manifests itself in infected cells. TA of CaMV is  
112 characterized by relocalization of CaMV particles and CaMV helper protein P2 from viral  
113 inclusions to microtubules (6, 10). Therefore, we performed immunofluorescence experiments on  
114 TuMV-infected protoplasts with antibodies directed against HC-Pro and the viral capsid protein  
115 CP to determine whether H<sub>2</sub>O<sub>2</sub> and LaCl<sub>3</sub> induced relocalization of TuMV virus particles and/or  
116 HC-Pro. In untreated cells, HC-Pro and CP localized in the cytoplasm as reported for other  
117 potyviruses (13, 14). Treatment with H<sub>2</sub>O<sub>2</sub> and LaCl<sub>3</sub> did not induce any visible rearrangement of  
118 HC-Pro or of CP (Figure 2). Thus, TA of TuMV is not characterized by the redistribution of  
119 HC-Pro and/or virus particles within infected cells.

120 We thus hypothesized that HC-Pro and virus particles, both evenly distributed in the cytoplasm,  
121 could pass from a non-associated state to an associated state, i.e. to transmissible HC-Pro-virion  
122 complexes, upon TA. To visualize such complexes *in situ*, we resorted to the Duolink® technique  
123 (15), an antibody-based version of the proximity ligation assay allowing detection of  
124 intermolecular interactions. Duolink® performed with HC-Pro and CP antibodies showed that  
125 H<sub>2</sub>O<sub>2</sub> treatment indeed increased the number and intensity of HC-Pro/CP interaction spots  
126 (Figure 3A,B), indicative of binding of HC-Pro to virus particles. Interestingly, incubation of  
127 protoplasts with LaCl<sub>3</sub> decreased the number of transmissible complexes (Figure 3C). Thus, the  
128 increase and decrease of HC-Pro/CP interactions, triggered by application of ROS or of a  
129 calcium channel blocker, respectively, correlated with an increase and decrease of transmission  
130 (compare Figures 1 and 3).

131 *Transmission activation of TuMV is characterized by formation of cysteine bridges between HC-Pro molecules*

132 We wanted to understand how HC-Pro and virus particles could rapidly transit from “free” to  
133 virus-associated forms. Since ROS like H<sub>2</sub>O<sub>2</sub> change directly or indirectly the cellular redox  
134 potential, the formation of HC-Pro/TuMV transmissible complexes might be controlled by the  
135 redox state of HC-Pro and CP, both of which contain cysteine residues that can form disulfide  
136 bridges under oxidizing conditions. Therefore, we performed non-reducing SDS-PAGE/Western  
137 blots to detect HC-Pro and CP migration profiles altered by intramolecular or intermolecular  
138 cysteine disulfide bridges. H<sub>2</sub>O<sub>2</sub> and LaCl<sub>3</sub> did not modify the migration profile of CP (Figure 4A).  
139 However, H<sub>2</sub>O<sub>2</sub> treatment increased the amount of oligomeric HC-Pro and especially of its

140 dimeric form (Figure 4B) that was previously reported to be active in transmission (16–18).  $\text{LaCl}_3$   
141 treatment had the inverse effect and decreased the amount of HC-Pro oligomers (Figure 4B).  
142 The effect of  $\text{H}_2\text{O}_2$  was concentration-dependent and clearly visible using physiologic  $\text{H}_2\text{O}_2$   
143 concentrations (0.25 mM, Figure 4C). Thus, the increase in transmission induced by  $\text{H}_2\text{O}_2$   
144 correlated not solely with formation of HC-Pro/TuMV complexes, but also with the appearance  
145 of HC-Pro oligomers hold together by intermolecular cysteine bridges.

146 To have a biological significance, HC-Pro oligomerization should be completed within the  
147 duration of an aphid puncture, i.e. within seconds. Kinetics of formation and breakup of HC-Pro  
148 oligomers showed that both occurred within 5 seconds of incubation with  $\text{H}_2\text{O}_2$  and  $\text{LaCl}_3$ ,  
149 respectively (Figure 4D,E). The effect of both treatments was transient because HC-Pro  
150 oligomers disappeared ( $\text{H}_2\text{O}_2$ ) or reappeared ( $\text{LaCl}_3$ ) after ~30 min incubation. Furthermore,  
151 removal of  $\text{H}_2\text{O}_2$  by washing protoplasts showed reversibility of HC-Pro oligomerization (Figure  
152 4D). Induction of HC-Pro oligomers by  $\text{H}_2\text{O}_2$  was not restricted to TuMV or to turnip hosts,  
153 because experiments with lettuce protoplasts infected with another potyvirus, *Lettuce mosaic virus*,  
154 yielded similar results (not shown).

155 To better establish that formation of disulfide bridges between HC-Pro monomers contributes to  
156 oligomerization, infected protoplasts were treated with the disulfide bonds-reducing agent  
157 dithiothreitol (DTT) or with N-ethylmaleimide (NEM) that does not break existing disulfide  
158 bridges but prevents formation of new ones by blocking free thiols. Figure 4F shows that DTT  
159 treatment abolished appearance of  $\text{H}_2\text{O}_2$ -induced HC-Pro oligomers in SDS-PAGE/Western  
160 blot. This confirmed that oligomerization of HC-Pro requires establishment of intermolecular  
161 disulfide bridges. NEM treatment blocked the appearance of HC-Pro oligomers in SDS-  
162 PAGE/Western blots when applied before the  $\text{H}_2\text{O}_2$  treatment, but NEM did not prevent their  
163 appearance when applied after  $\text{H}_2\text{O}_2$  treatment (Figure 4G). This is a further confirmation of the  
164 involvement of disulfide bridges in HC-Pro oligomerization. Note that NEM treatment caused a  
165 mobility shift of HC-Pro. This might have been due to disulfide shuffling during denaturation of  
166 the samples as reported for papilloma virus (19). To establish a direct role of intermolecular HC-  
167 Pro disulfide bonds in TuMV transmission, we performed transmission assays. Because of the  
168 toxicity of NEM, we did not use plants as virus source but resorted to the protoplast system  
169 where exposure of aphids (and the experimenter) to the substance is minimized by confining it in  
170 the protoplast medium. The NEM treatment reduced virus transmission drastically (Figure 4H)  
171 but did not affect protoplast viability (Figure 4I), suggesting that *de novo* formation of

172 intermolecular HC-Pro disulfide bonds is required for formation of transmissible complexes and  
173 thus for aphid acquisition of TuMV.

174 *Model of TuMV transmission activation*

175 In this study, we demonstrate that TA exists for a second virus, TuMV. TuMV TA was induced  
176 by the ROS H<sub>2</sub>O<sub>2</sub> and inhibited by the calcium channel blocker LaCl<sub>3</sub>. ROS and calcium signaling  
177 are both important in early perception of parasites including insects (20) and recently aphid  
178 punctures were described to induce rapid calcium elevations around feeding sites (21). Since ROS  
179 and calcium signaling are often interconnected (22, 23), TuMV TA likely hijacks an early step of  
180 at least one of these pathways. The initial eliciting event remains unknown. It might be a direct  
181 effect of aphid saliva-contained ROS or ROS-producing peroxidases (24) that are injected into  
182 cells during feeding activity. Alternatively, an aphid or aphid-induced plant factor might interact  
183 in a classic pathogen-associated molecular pattern (PAMP)-triggered immunity reaction with a  
184 pattern recognition receptor (PRR) (25) that prompts calcium and ROS mediated downstream  
185 events. Interestingly, a recent study has demonstrated that the red clover necrotic mosaic virus  
186 (RCNMV) requires ROS for replication (26). The authors proposed that plant viruses may have  
187 evolved a complex mechanism to manipulate the ROS-generating machinery of plants to  
188 improve their infectivity, or, transferred to this case, transmission.

189 TA of TuMV manifests itself by creation of HC-Pro intermolecular disulfide bridges, driven by  
190 oxidation of the cellular redox potential. We propose that oxidation of HC-Pro induces a  
191 functional switch rendering HC-Pro able to interact with virus particles and form transmissible  
192 complexes (Figure 5). Functional switching (moonlighting) by redox-driven modification of  
193 disulfide bridges has been reported for other proteins and is operated by conformation changes  
194 affecting the secondary, tertiary or quaternary structure of proteins (27–29). Why would there be  
195 such a switch? HC-Pro is a multifunctional protein involved not only in aphid transmission (30)  
196 but also in pathogenicity (31), viral movement (32) and suppression of plant RNA silencing (33–  
197 35). One (or more) functional switches could assist to coordinate these multiple functions by  
198 allowing interaction with virions and formation of transmissible complexes only when  
199 transmission is possible, i.e. when the aphids puncture cells This would help to economize finite  
200 plant resources as proposed earlier (7).

201 Unfortunately, we cannot provide an empirical proof that the aphid punctures directly trigger  
202 TuMV TA. In contrast to CaMV, where TA was directly visible using qualitative  
203 immunofluorescence observation of P2 and virus particle networks (the characteristic

204 manifestation of CaMV TA) in cells in contact with aphid saliva sheaths, TuMV TA cannot be  
205 revealed by a qualitative analysis. The quantitative Duolink® approach we used to demonstrate  
206 TuMV HC-Pro/CP interactions in protoplasts required an enormous number of cells for analysis  
207 and statistical validation. Identifying a comparable number of cells in tissue and in contact with  
208 aphid stylets is barely feasible. The same restrictions apply to electron microscopy techniques to  
209 localize HC-Pro on virus particles by immunogold labeling. Thus, proof of aphid implication in  
210 TA of TuMV remains indirect, for the time being.

211 Nonetheless, we here demonstrate TA for a second virus, TuMV, different from CaMV,  
212 suggesting that transmission activation might be a more general phenomenon. The great  
213 phylogenetic distance between TuMV and CaMV makes it likely that the phenomenon of TA  
214 arose independently for the two viruses during evolution. An obvious question is whether yet  
215 other viruses use TA for their transmission.

## 216 **Materials and methods**

### 217 Plants, viruses and inoculation

218 Turnip plants (*Brassica rapa* cv. Just Right) and lettuce (*Lactuca sativa* cv. Mantilla and Trocadero)  
219 were grown in a greenhouse at 24/15 °C day/night with a 14/10 h day/night photoperiod. Two-  
220 weeks-old turnip plants were mechanically inoculated with wild-type TuMV strain C42J (36), and  
221 two-weeks-old lettuce plants with *Lettuce mosaic virus* (LMV) strain E (37). Plants were used for  
222 experiments at 14 days post inoculation (dpi).

### 223 Isolation of protoplasts

224 Protoplasts from turnip leaves were obtained by enzymatic digestion as described (6).

### 225 Preparation of infected cell extracts

226 TuMV-infected turnip protoplasts were sedimented and resuspended in SAKO buffer (500 mM  
227 KPO<sub>4</sub> and 10 mM MgCl<sub>2</sub> pH 8.5) (38). Then sucrose was added to a final concentration of 15 %  
228 and the suspension was vortexed to homogenize protoplasts.

### 229 Drug treatments and cell viability assay

230 For drug treatments of protoplasts, the following substances were added from stock solutions for  
231 the indicated times to 500 µl of protoplast suspension: 1 mM LaCl<sub>3</sub> (5 min), 2 mM H<sub>2</sub>O<sub>2</sub> (5 min),

232 3 mM NEM (20 min), 5 mM DTT (30 min). Protoplasts were incubated at room temperature  
233 with gentle stirring (5 rpm). 15 min after treatments, protoplast viability was determined with the  
234 FDA test (39). For drug treatments of plants, one leaf per plant was sprayed with 10 mM LaCl<sub>3</sub>,  
235 20 mM H<sub>2</sub>O<sub>2</sub> or with water, and the leaf, still attached to the plant, used for transmission  
236 experiments after the applied solutions had evaporated.

#### 237 Aphid transmission tests

238 A nonviruliferous clonal *Myzus persicae* colony was reared under controlled conditions (22/18 °C  
239 day/night with a photoperiod of 14/10 h day/night) on eggplant. The transmission tests using  
240 protoplasts were performed as described (6), with an acquisition access period of 15 min and  
241 transferring 10 aphids to each test plant. For plant-to-plant transmission tests, an acquisition time  
242 of 2 min was used and only one aphid was transferred on each turnip plant for inoculation.  
243 Infected plants were identified by visual inspection for symptoms 3 weeks after inoculation.

#### 244 Antisera

245 The following primary antibodies were used: commercial rabbit anti-TuMV (sediag.com) and  
246 mouse and rabbit anti-HC-Pro (recognizing HC-Pro from different potyviruses, produced against  
247 the conserved peptide SEIKMPTKHHHLVIGNSGDPKYIDL P by proteogenix.fr and  
248 eurogentec.com, respectively). The following secondary antibodies were used: Alexa Fluor 488  
249 and 594 anti-rabbit and anti-mouse conjugates (thermofisher.com) for immunofluorescence, anti-  
250 rabbit IgG conjugated to alkaline phosphatase (www.sigmaaldrich.com) for western blotting and  
251 corresponding Minus and Plus probes (www.sigmaaldrich.com) for Duolink®.

#### 252 Immunofluorescence

253 Protoplasts were fixed with 1 % glutaraldehyde and processed as described (6). The primary and  
254 secondary antibodies were used at 1:100 and 1:200 dilutions, respectively.

#### 255 Western blotting

256 Drug treatments of protoplasts were stopped by lysing protoplasts in non-reducing 2x Laemmli  
257 buffer (v/v) (40) except where indicated otherwise. Optionally, oligomer formation was stabilized  
258 by incubating protoplasts with 3 mM NEM for 20 min before lysis. This step yielded sharper  
259 oligomer bands. Samples were then resolved by 10 % SDS-PAGE. Proteins were transferred to  
260 nitrocellulose membranes and incubated with primary and secondary antibodies as described (6)

261 except that TuMV-specific primary antibodies (1:1000 dilution) were used. Antigens were then  
262 revealed by the NBT/BCIP reaction. Equal protein charge on the membranes was verified by  
263 coloring the RuBisCO with Ponceau S Red.

#### 264 Duolink® proximity ligation assay

265 *In situ* protein/protein interactions were detected by proximity ligation assay using the Duolink®  
266 kit (www.sigmaaldrich.com). Protoplasts were isolated from healthy or infected (14 dpi) turnip  
267 leaves and fixed with 3 % paraformaldehyde in 100 mM cacodylate buffer (pH 7.2) or 100 mM  
268 phosphate buffer (pH 7.4). The fixed protoplasts were immobilized on L-polylysine-coated slides.  
269 Antibody incubation with rabbit anti-TuMV and mouse anti-HC-Pro, ligation and probe  
270 amplification were performed according to the manufacturer's instructions. The slides were  
271 mounted with Duolink® *in situ* mounting medium with DAPI (www.sigmaaldrich.com).

#### 272 Microscopy

273 Immunolabeled protoplasts were observed with an Olympus BX60 epifluorescence microscope  
274 (olympus-lifescience.com) equipped with GFP and Texas Red narrow band filters and images  
275 acquired with a color camera. Duolink® images were acquired with a Zeiss LSM700 confocal  
276 microscope (zeiss.com) operated in sequential mode. DAPI was excited with the 405 nm laser and  
277 fluorescence collected from 405-500 nm, Duolink® probes and chlorophyll were excited with the  
278 488 nm laser and fluorescence collected from 490-540 nm (Duolink® signal) or from 560-735 nm  
279 (chlorophyll autofluorescence). Raw images were processed using ZEN or ImageJ software.  
280 Quantification of Duolink® interactions was performed on maximum intensity projections with  
281 the Analyse\_Spots\_Per\_Protoplast macro for ImageJ, developed for this experiment (41).

#### 282 Statistical analysis

283 Statistics and box plots were calculated with R software version 3.4.0 (r-project.org).  
284 Transmission rates and cell viability were analyzed with generalized linear models (GLM). Quasi-  
285 binomial distributions were used in order to take overdispersion into account, and p-values were  
286 corrected with the Holm method (42) to account for multiple comparisons.

287 Analyzing the Duolink® experiments required the calculation of the total fluorescence intensity  
288 ( $F_{tot}$ ) of labeled foci as:

289

290 
$$F_{tot} = \frac{n \times \bar{s} \times \bar{I}}{A}$$

291

292 where  $n$  is the number of labeled foci,  $\bar{s}$  the average size of a focus,  $\bar{I}$  the average fluorescence  
293 intensity of a focus and  $A$  the size of the protoplast.  $F_{tot}$  was log-transformed (to normalize the  
294 distribution) and analyzed with linear models using “treatment” and “replicate” as categorical  
295 explanatory variables.

## 296 References

- 297 1. Blanc S, Drucker M, Uzest M. 2014. Localizing viruses in their insect vectors. *Annu Rev*  
298 *Phytopathol* 52:403–425.
- 299 2. Dáder B, Then C, Berthelot E, Ducouso M, Ng JCK, Drucker M. 2017. Insect transmission of  
300 plant viruses: Multilayered interactions optimize viral propagation. *Insect Sci* 24:929–946.
- 301 3. Kuno G, Chang G-JJ. 2005. Biological transmission of arboviruses: reexamination of and new  
302 insights into components, mechanisms, and unique traits as well as their evolutionary trends. *Clin*  
303 *Microbiol Rev* 18:608–637.
- 304 4. Lefèvre T, Adamo SA, Biron DG, Missé D, Hughes D, Thomas F. 2009. Invasion of the body  
305 snatchers: the diversity and evolution of manipulative strategies in host-parasite interactions. *Adv*  
306 *Parasitol* 68:45–83.
- 307 5. Matthews KR. 2011. Controlling and coordinating development in vector-transmitted parasites.  
308 *Science* 331:1149–1153.
- 309 6. Martinière A, Bak A, Macia J-L, Lautredou N, Gargani D, Doumayrou J, Garzo E, Moreno A,  
310 Fereres A, Blanc S, Drucker M. 2013. A virus responds instantly to the presence of the vector on the  
311 host and forms transmission morphs. *eLife* 2:e00183.
- 312 7. Drucker M, Then C. 2015. Transmission activation in non-circulative virus transmission: a general  
313 concept? *Curr Opin Virol* 15:63–68.

- 314 8. Drucker M, Froissart R, Hébrard E, Uzeš M, Ravallec M, Espérandieu P, Mani J-C, Pugnère M,  
315 Roquet F, Fereres A, Blanc S. 2002. Intracellular distribution of viral gene products regulates a  
316 complex mechanism of cauliflower mosaic virus acquisition by its aphid vector. *Proc Natl Acad Sci*  
317 *USA* 99:2422–2427.
- 318 9. Espinoza AM, Medina V, Hull R, Markham PG. 1991. Cauliflower mosaic virus gene II product  
319 forms distinct inclusion bodies in infected plant cells. *Virology* 185:337–344.
- 320 10. Bak A, Gargani D, Macia J-L, Malouvet E, Vernerey M-S, Blanc S, Drucker M. 2013. Virus factories  
321 of Cauliflower mosaic virus are virion reservoirs that engage actively in vector-transmission. *J Virol.*
- 322 11. Martinière A, Macia J-L, Bagnolini G, Jridi C, Bak A, Blanc S, Drucker M. 2011. VAPA, an  
323 Innovative “Virus-Acquisition Phenotyping Assay” Opens New Horizons in Research into the  
324 Vector-Transmission of Plant Viruses. *PLoS One* 6.
- 325 12. Peng H-C, Walker GP. 2018. Sieve element occlusion provides resistance against *Aphis gossypii* in  
326 TGR-1551 melons. *Insect Sci.*
- 327 13. Baunoch DA, Das P, Hari V. 1990. Potato virus Y helper component protein is associated with  
328 amorphous inclusions. *J Gen Virol* 71 ( Pt 10):2479–2482.
- 329 14. Riedel D, Lesemann DE, Maiss E. 1998. Ultrastructural localization of nonstructural and coat  
330 proteins of 19 potyviruses using antisera to bacterially expressed proteins of plum pox potyvirus.  
331 *Arch Virol* 143:2133–2158.
- 332 15. Söderberg O, Gullberg M, Jarvius M, Ridderstråle K, Leuchowius K-J, Jarvius J, Wester K,  
333 Hydbring P, Bahram F, Larsson L-G, Landegren U. 2006. Direct observation of individual  
334 endogenous protein complexes in situ by proximity ligation. *Nat Methods* 3:995–1000.
- 335 16. Plisson C, Drucker M, Blanc S, German-Retana S, Le Gall O, Thomas D, Bron P. 2003. Structural  
336 characterization of HC-Pro, a plant virus multifunctional protein. *J Biol Chem* 278:23753–23761.

- 337 17. Ruiz-Ferrer V, Boskovic J, Alfonso C, Rivas G, Llorca O, López-Abella D, López-Moya JJ. 2005.  
338 Structural analysis of tobacco etch potyvirus HC-pro oligomers involved in aphid transmission. *J*  
339 *Virology* 79:3758–3765.
- 340 18. Thornbury DW, Hellmann GM, Rhoads RE, Pirone TP. 1985. Purification and characterization of  
341 potyvirus helper component. *Virology* 144:260–267.
- 342 19. Modis Y, Trus BL, Harrison SC. 2002. Atomic model of the papillomavirus capsid. *EMBO J*  
343 21:4754–4762.
- 344 20. Zebelo SA, Maffei ME. 2015. Role of early signalling events in plant-insect interactions. *J Exp Bot*  
345 66:435–448.
- 346 21. Vincent TR, Avramova M, Canham J, Higgins P, Bilkey N, Mugford ST, Pitino M, Toyota M,  
347 Gilroy S, Miller AJ, Hogenhout SA, Sanders D. 2017. Interplay of Plasma Membrane and Vacuolar  
348 Ion Channels, Together with BAK1, Elicits Rapid Cytosolic Calcium Elevations in Arabidopsis  
349 during Aphid Feeding. *Plant Cell* 29:1460–1479.
- 350 22. Jeworutzki E, Roelfsema MRG, Anschutz U, Krol E, Elzenga JTM, Felix G, Boller T, Hedrich R,  
351 Becker D. 2010. Early signaling through the Arabidopsis pattern recognition receptors FLS2 and  
352 EFR involves Ca-associated opening of plasma membrane anion channels. *Plant J* 62:367–378.
- 353 23. Lachaud C, Da Silva D, Amelot N, Béziat C, Brière C, Cotelle V, Graziana A, Grat S, Mazars C,  
354 Thuleau P. 2011. Dihydrosphingosine-induced programmed cell death in tobacco BY-2 cells is  
355 independent of H<sub>2</sub>O<sub>2</sub> production. *Mol Plant* 4:310–318.
- 356 24. Miles PW. 1999. Aphid Saliva. *Biological Reviews* 74:41–85.
- 357 25. Jones JDG, Dangl JL. 2006. The plant immune system. *Nature* 444:323–329.
- 358 26. Hyodo K, Hashimoto K, Kuchitsu K, Suzuki N, Okuno T. 2017. Harnessing host ROS-generating  
359 machinery for the robust genome replication of a plant RNA virus. *Proc Natl Acad Sci USA*  
360 114:E1282–E1290.

- 361 27. Fan SW, George RA, Haworth NL, Feng LL, Liu JY, Wouters MA. 2009. Conformational changes  
362 in redox pairs of protein structures. *Protein Sci* 18:1745–1765.
- 363 28. Mou Z, Fan W, Dong X. 2003. Inducers of plant systemic acquired resistance regulate NPR1  
364 function through redox changes. *Cell* 113:935–944.
- 365 29. Zaffagnini M, Fermani S, Costa A, Lemaire SD, Trost P. 2013. Plant cytoplasmic GAPDH: redox  
366 post-translational modifications and moonlighting properties. *Front Plant Sci* 4:450.
- 367 30. Govier DA, Kassanis B. 1974. A virus induced component of plant sap needed when aphids acquire  
368 potato virus Y from purified preparations. *Virology* 61:420–426.
- 369 31. Atreya CD, Atreya PL, Thornbury DW, Pirone TP. 1992. Site-directed mutations in the potyvirus  
370 HC-Pro gene affect helper component activity, virus accumulation, and symptom expression in  
371 infected tobacco plants. *Virology* 191:106–111.
- 372 32. Cronin S, Verchot J, Haldeman-Cahill R, Schaad MC, Carrington JC. 1995. Long-distance  
373 movement factor: a transport function of the potyvirus helper component proteinase. *Plant Cell*  
374 7:549–559.
- 375 33. Anandalakshmi R, Marathe R, Ge X, Herr JM, Mau C, Mallory A, Pruss G, Bowman L, Vance VB.  
376 2000. A calmodulin-related protein that suppresses posttranscriptional gene silencing in plants.  
377 *Science* 290:142–4.
- 378 34. Brigneti G, Voinnet O, Li WX, Ji LH, Ding SW, Baulcombe DC. 1998. Viral pathogenicity  
379 determinants are suppressors of transgene silencing in *Nicotiana benthamiana*. *EMBO J* 17:6739–  
380 6746.
- 381 35. Kasschau KD, Carrington JC. 1998. A counterdefensive strategy of plant viruses: suppression of  
382 posttranscriptional gene silencing. *Cell* 95:461–70.

- 383 36. Ohshima K, Tomitaka Y, Wood JT, Minematsu Y, Kajiyama H, Tomimura K, Gibbs AJ. 2007.  
384 Patterns of recombination in turnip mosaic virus genomic sequences indicate hotspots of  
385 recombination. *J Gen Virol* 88:298–315.
- 386 37. Revers F, Yang SJ, Walter J, Souche S, Lot H, Le Gall O, Candresse T, Dunez J. 1997. Comparison  
387 of the complete nucleotide sequences of two isolates of lettuce mosaic virus differing in their  
388 biological properties. *Virus Res* 47:167–177.
- 389 38. Sako N, Ogata K. 1981. Different helper factors associated with aphid transmission of some  
390 potyviruses. *Virology* 112:762–765.
- 391 39. Widholm JM. 1972. The use of fluorescein diacetate and phenosafranine for determining viability of  
392 cultured plant cells. *Stain Technol* 47:189–194.
- 393 40. Laemmli UK. 1970. Cleavage of Structural Proteins during the Assembly of the Head of  
394 Bacteriophage T4. *Nature* 227:680–685.
- 395 41. Baecker V. 2016. Analyse Spots Per Protoplast - ImageJ-macros - MRI's Redmine.
- 396 42. Holm S. 1979. A simple sequentially rejective multiple test procedure. *Scand J Statist* 6:65–70.
- 397 43. Bak A, Martinière A, Blanc S, Drucker M. 2013. Early interactions during the encounter of plants,  
398 aphids and arboviruses. *Plant Signal Behav* 8:e24225.

### 399 **Acknowledgments**

400 We are grateful to Takii Europe for providing turnip seeds. Our work is financed by INRA SPE  
401 department, Agence Nationale de la Recherche (ANR) grant 12-BSV7-005-01, awarded to MD,  
402 and grant RGP0013/2015 from Human Frontier Science Program (HFSP), awarded to MD. EB  
403 is supported by CIFRE PhD fellowship N° 2015/1115, financed by Association Nationale  
404 Recherche Technologie (anrt), Semences Innovation Protection Recherche et Environnement  
405 (SIPRE) and Fédération Nationale des Producteurs de Plantes de Pomme de Terre (FN3PT). We  
406 thank Albin Teulet for help with the box plots and Sophie Le Blaye for plant care. All authors  
407 declare that there is no conflict of interest.

408 **Legends to Figures**

409 **Figure 1.** Effect of H<sub>2</sub>O<sub>2</sub> and LaCl<sub>3</sub> on TuMV transmission by aphids. (A-B) Turnip protoplasts  
410 were incubated for 5 min with 2 mM H<sub>2</sub>O<sub>2</sub> (A) or 1 mM LaCl<sub>3</sub> (B) and then employed in  
411 transmission assays. (C-D) Cell viability of protoplasts was measured to determine if the altered  
412 transmission rates were due to modified viability. (E-F) Cell extracts from protoplasts were  
413 treated identically with H<sub>2</sub>O<sub>2</sub> (C) or LaCl<sub>3</sub> (D) and used in transmission assays. (G-H) Leaves on  
414 intact plants were sprayed with 20 mM H<sub>2</sub>O<sub>2</sub> (E) or 10 mM LaCl<sub>3</sub> (F) and then employed in  
415 transmission assays. Means of infected test plants (horizontal black bars in the box plots) are  
416 calculated from a pool of three independent experiments in which a total of 360 tests plants were  
417 used per condition. Each experiment had 6 repetitions for each condition and 20 tests plants per  
418 repetition (see Supplementary Data Set S1 for raw data). *p* designates p-values obtained by  
419 generalized linear models (see materials and methods). The box plots here and in the other  
420 figures present medians, upper and lower quartiles, the ends of the whiskers present lowest and  
421 highest datum still within 1.5 IQR of the lower and higher quartile, respectively, and the circles  
422 show outliers.

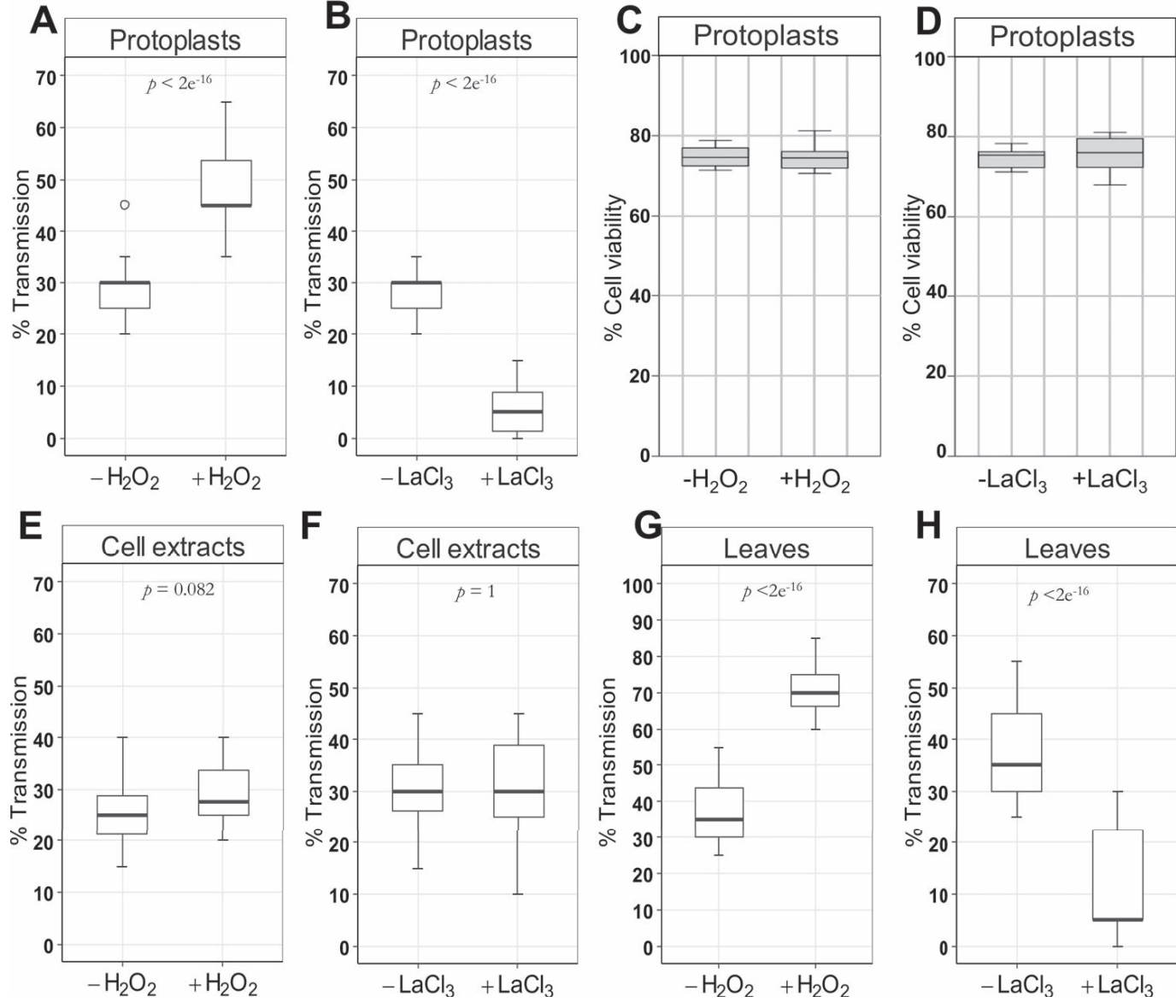
423 **Figure 2.** Immunofluorescence of turnip protoplasts infected with TuMV. TuMV-infected  
424 protoplasts were treated as indicated and double-labeled against HC-Pro (green, first column) and  
425 viral capsid protein CP (red, middle column). The right column (Merge) represents superposition  
426 of HC-Pro and CP labels, with co-labeling appearing in yellow. Control, untreated protoplasts;  
427 H<sub>2</sub>O<sub>2</sub>, incubation with 2 mM H<sub>2</sub>O<sub>2</sub> for 15 min, LaCl<sub>3</sub>, incubation with 1 mM LaCl<sub>3</sub> for 15 min.  
428 Scale bars 50 μm.

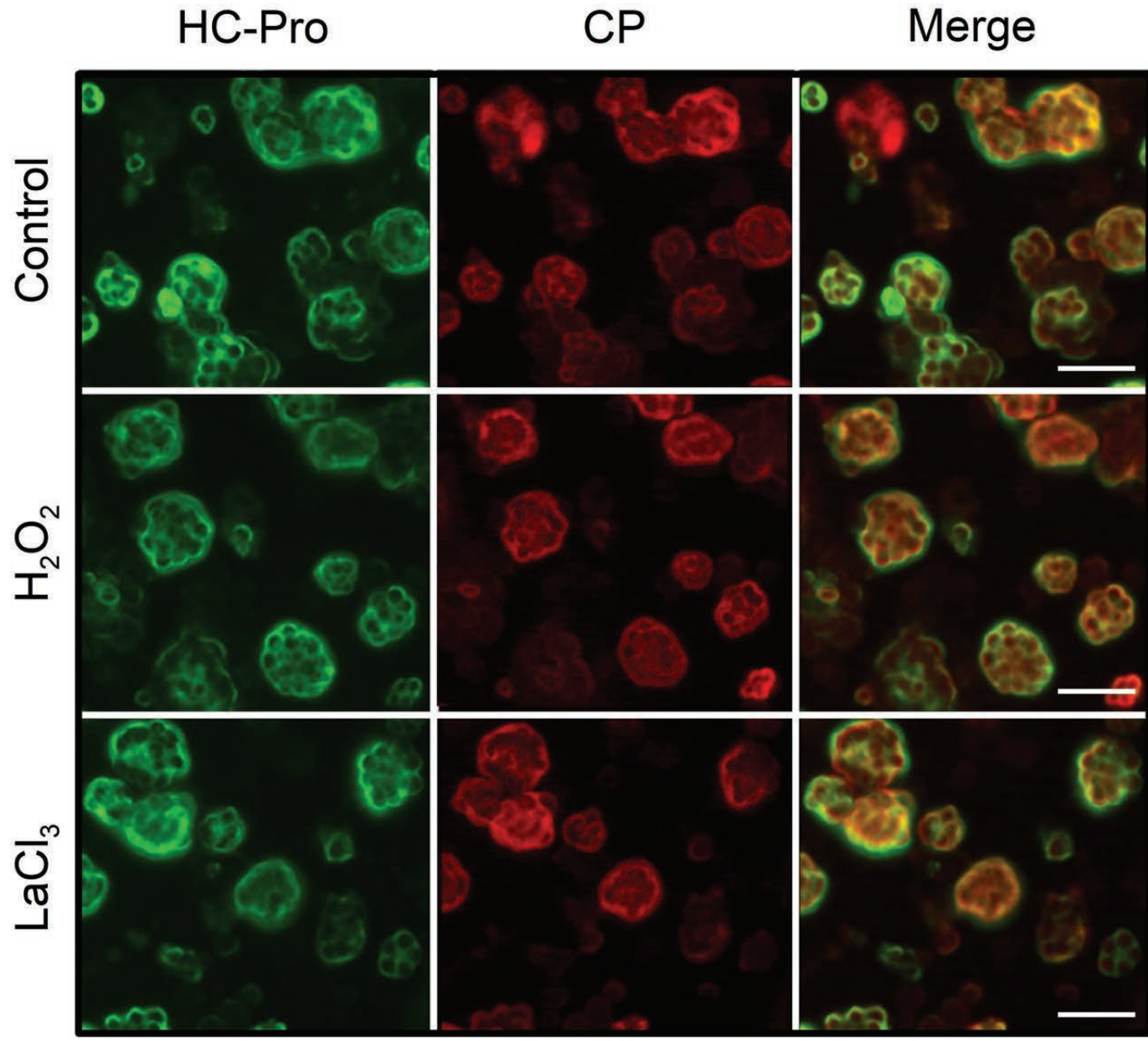
429 **Figure 3.** *In situ* Duolink® proximity ligation assay on turnip protoplasts infected with TuMV.  
430 (A) Untreated control protoplasts or protoplasts incubated with either H<sub>2</sub>O<sub>2</sub> or LaCl<sub>3</sub> were  
431 processed by Duolink® for detection of HC-Pro/TuMV particle interactions using HC-Pro and  
432 CP antibodies and corresponding Duolink® probes. Interactions are visible as green fluorescing  
433 spots. Nuclei were counterstained with DAPI (blue) and chloroplast autofluorescence is  
434 presented in grey to reveal the cell lumen. Scale bars: 20 μm. (B-C) Quantitative analysis of the  
435 Duolink® signal shows that (B) H<sub>2</sub>O<sub>2</sub> increased and (C) LaCl<sub>3</sub> decreased HC-Pro/CP interactions.  
436 The box plots presents data from three independent experiments using between 56-115  
437 protoplasts for each condition. The y-axes show HC-Pro/CP interactions, presented as total  
438 fluorescent intensity ( $F_{int}$ ). *p* designates p -values obtained by generalized linear models (see  
439 material and methods).

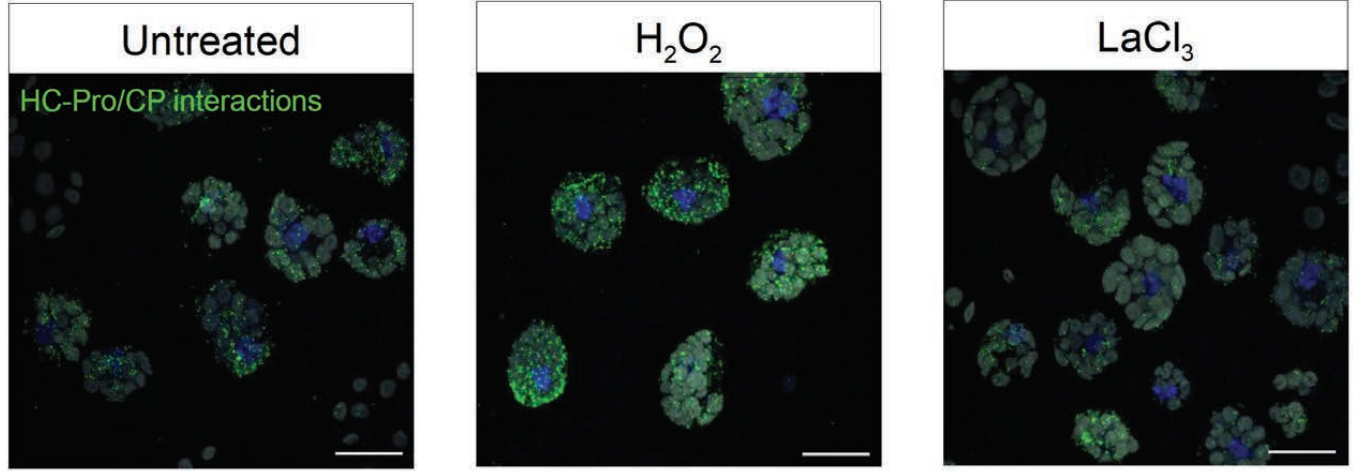
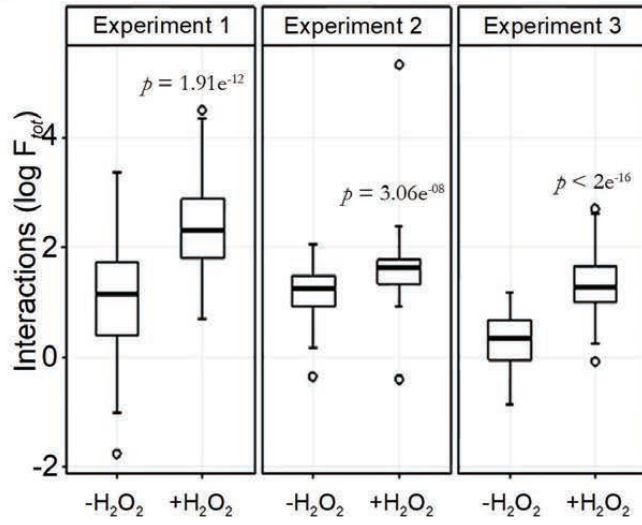
440 **Figure 4.** Non-reducing SDS-PAGE/Western blotting analysis of HC-Pro and CP from TuMV-  
441 infected turnip protoplasts. The samples were lysed in a buffer without reducing agents to  
442 conserve the disulfide bridges. (A)  $H_2O_2$  and  $LaCl_3$  treatments did not modify the migration  
443 profile of the capsid protein (CP), whereas they (B) induced ( $H_2O_2$ ) or inhibited ( $LaCl_3$ )  
444 formation of HC-Pro oligomers. (C-D) The concentration range and the kinetics of  $H_2O_2$   
445 incubation shows that HC-Pro oligomerization (C) was induced by a minimum concentration of  
446 0.25 mM and (D) that it was rapid and reversible, either by extended  $H_2O_2$  treatment (left panel)  
447 or by washing protoplasts (right panel). (E) Also inhibition of HC-Pro oligomerization by  $LaCl_3$   
448 was rapid and reversible. (F-G) HC-Pro oligomers are formed by intermolecular disulfide bridges  
449 because (F) incubation of protoplasts with DTT, either alone or after  $H_2O_2$  treatment, abolished  
450 HC-Pro oligomers, and (G) treatment with NEM before but not after previous incubation with  
451  $H_2O_2$  prevented their formation. (H) Transmission tests using NEM-treated protoplasts show a  
452 drastic diminution of TuMV transmission. Transmission tests were performed three times using  
453 320 plants per condition and analyzed by generalized linear models as described in Figure 1. (I)  
454 Protoplast viability assays show that NEM treatment did not change cell viability under the  
455 conditions used. TuMV, samples of TuMV-infected protoplasts; Non inf., samples of non  
456 infected protoplasts;  $LaCl_3$ , treatment with 1 mM  $LaCl_3$  for 5 min;  $H_2O_2$ , treatment with 2 mM  
457  $H_2O_2$  for 5 min; wash,  $H_2O_2$  was removed by centrifugation and resuspension of protoplasts in  
458 fresh medium; DTT, treatment with 5 mM DTT for 30 min; NEM, treatment with 3 mM NEM  
459 for 20 min. Equal loading of lanes is shown by Ponceau Red staining of the large RuBisCO  
460 subunit (Rub). A precolored ladder and the molecular masses in kDa are indicated at one side of  
461 each blot.  $p$  in (H) designates p-value obtained by generalized linear models from three  
462 independent experiments.

463 **Figure 5.** Model of TuMV acquisition by aphids. For simplicity, aphids, viral components and  
464 the plant cell are not drawn to scale. (1) Before the arrival of aphid vectors, the redox potential of  
465 the cytosol of TuMV-infected cells has ‘normal’ values, i.e. it is reduced. Consequently, the  
466 cytosolic HC-Pro protein (blue circles) is in a reduced form (the red points in HC-Pro present  
467 reduced cysteines) and contains no intermolecular disulfide bridges. This form of HC-Pro is  
468 presumably not associated with virus particles (purple lines). It is likely but remains to be  
469 confirmed whether reduced HC-Pro is dimeric as presented here. (2) When an aphid feeds on a  
470 leaf infected with TuMV, an unknown elicitor is recognized by the plant cell and induces the  
471 opening of calcium channels (pink cylinder) and triggers directly or indirectly ROS production in  
472 the cell. During this activation stage, the ROS in the cytoplasm increases (red lightning) the redox  
473 potential of the cell cytoplasm and oxidizes one or more HC-Pro cysteines. This oxidation

474 generates disulfide bridges (red lines) between different HC-Pro molecules. The intermolecular  
475 disulfide bridges either induce oligomerization of a portion of HC-Pro or change the  
476 conformation of a part of existing oligomers, presented by the transition of the circles to squares.  
477 For simplicity, higher HC-Pro forms are not shown. (3) Whatever the case, oxidation of a  
478 fraction of HC-Pro results in a functional switch of the protein and the oxidized tertiary or  
479 quaternary conformation allows interaction between HC-Pro and TuMV particles and the  
480 formation of TuMV transmissible complexes, symbolized by square HC-Pro aligned with a virion.  
481 Now the infected cell is switched into transmission mode and this stage allows efficient  
482 acquisition of TuMV. (4) The aphid acquires transmissible complexes and transmits the TuMV  
483 during the next punctures on another plant. After vector departure, the redox potential of cell  
484 cytoplasm lowers again and HC-Pro is reduced. This changes its conformation and induces  
485 dissociation of the transmissible complexes, leaving HC-Pro free to fulfill its other functions  
486 during infection. The aphid drawing is modified from (43), published under open CC3.0 license.





**A****B****C**